Global Decarbonisation | Volume 2 (2026) | ISSN 3050-0230

Publish open access at Caravel Press

Global Decarbonisation

Journal homepage: globaldecarbonisation.com

Technical article

Dynamical Analysis and Control of a Carbon Credit Investment System with Chaotic Behavior and Fractional-Order Memory

Sofia E. Krzyuy [1]*, Giane G. Lenzi [2], Maria E. K. Fuziki [2], Jose M. Balthazar [3], Leda M. S. Colpini [4], Onelia A. A. dos Santos [5] and Angelo M. Tusset [1]

[1] *Department of Production Engineering, Federal University of Technology – Paraná (UTFPR), Ponta Grossa, Paraná, Brazil*
[2] *Department of Chemical Engineering, Federal University of Technology – Paraná (UTFPR), Ponta Grossa, Paraná, Brazil*
[3] *Department of Mechanical Engineering, São Paulo State University (UNESP), Bauru, São Paulo, Brazil*
[4] *Federal University of Paraná (UFPR), Jandaia do Sul, Paraná, Brazil*
[5] *State University of Maringá (UEM), Maringá, Brazil*

ABSTRACT

This study investigates the dynamic behavior of a carbon credit investment system using nonlinear analysis, fractional-order modeling, and active control techniques. The analysis focuses on parameters associated with the demand for green investments and the impact of the carbon tax rate. System dynamics are characterized through bifurcation diagrams, phase portraits, time series, and Lyapunov exponents, enabling the identification of distinct dynamic regimes, including periodic and chaotic behaviors. To incorporate memory effects inherent in economic variables, fractional-order formulations based on the Riemann–Liouville operator are employed, revealing that the order of the fractional derivative significantly influences the system's dynamics. To stabilize the system and suppress chaotic behavior, a linear controller of the Linear Quadratic Regulator (LQR) type and a nonlinear controller based on the State-Dependent Riccati Equation (SDRE) are designed. The results demonstrate that both strategies successfully drive the system toward desired equilibrium states while exhibiting low tracking errors. Furthermore, addressing scenarios where not all state variables are directly available for feedback, state observers are utilized to estimate unmeasured variables and supply the necessary information to the controllers. The findings provide a quantitative basis for understanding the complex dynamics associated with carbon credit investments and highlight the applicability of control strategies for system stabilization and the mitigation of undesirable dynamic behaviors.

ARTICLE INFO

Article History:
Received: 09 June 2026
Revised: 13 August 2026
Accepted: 27 August 2026

Keywords:
Carbon credits
Chaotic financial system
LQR control
SDRE control
Dynamical analysis

Article Citation:
{leave blank}

1. INTRODUCTION

Initially conceived under the 1997 Kyoto Protocol, carbon credits were designed as an innovative market-based mechanism to facilitate the trading of emission reductions between countries and corporations (Zhen *et al.*, 2026). Since then, environmental policy has evolved significantly beyond traditional regulatory frameworks to embrace these instruments, positioning green credit initiatives at the core of global climate

* Corresponding author. Email address: sofiakrzyuy@alunos.utfpr.edu.br (Sofia E. Krzyuy)

finance, as documented by Okolo *et al*. (2026). Given the current urgency of mitigating greenhouse gas (GHG) emissions, these markets are now recognized as indispensable tools for achieving international sustainable development goals (Xu *et al*., 2023).

Beyond mandatory frameworks, carbon credits have flourished in voluntary markets, serving a dual purpose: mitigating climate change while fostering corporate sustainability. However, their effectiveness and credibility remain contingent upon their integration into robust policy frameworks and transparent institutional structures, as emphasized by Cariappa *et al*. (2024) and Rigo *et al*. (2026). In this context, recent empirical evidence underscores the role of market-based environmental instruments in reducing emissions across diverse sectors. Notably, Zhang *et al*. (2025) demonstrate that green financial instruments, closely related in design to carbon pricing mechanisms, can significantly reduce the carbon emission intensity of enterprises, both at the macro level, through industrial structure upgrading and energy efficiency improvement, and at the micro level, by reshaping corporate investment behavior and reducing inefficient capital allocation.

This intersection between environmental governance and financial logic becomes particularly salient when carbon is examined as an investable asset class, a framework formalized by Azlen *et al*. (2022), enabling a better understanding of how these markets can be leveraged to align environmental imperatives with economic objectives. Building on this perspective, Swinkels and Yang (2023) provide evidence that returns from the global carbon market offer meaningful diversification benefits for investors in conventional asset classes such as stocks, bonds, and commodities. The growing involvement of financial investors, multilateral institutions, and private capital markets in funding the energy transition further underscores the strategic role of finance in shaping sustainable development pathways (Xi *et al*., 2026). However, empirical tracking of climate finance flows in developing economies reveals a persistent gap between international pledges and capital disbursed, underscoring the practical fragility of these funding commitments (Verma, 2026). Extending this line of inquiry, Awuah *et al*. (2026) integrate economic attractiveness and carbon balances within a climate finance framework, offering actionable insights for navigating sustainable investment decisions, thereby bridging the gap between environmental accountability and capital allocation strategy. Yet, the very characteristics that render carbon markets financially attractive, their sensitivity to regulatory shifts, their exposure to global policy dynamics, and their dependence on environmental integrity, also make them inherently volatile and structurally difficult to predict.

Indeed, investments in carbon credits occur within highly complex financial and environmental systems characterized by profound uncertainty, which poses a critical challenge for decision-support and asset management standards (Zambujal-Oliveira and Duque, 2026). Johansyah *et al*. (2026) emphasize that such chaotic dynamics manifest through the inherent unpredictability and volatility of economic variables, elucidating how minor perturbations can propagate into systemic crises and why arbitrage opportunities tend to arise and dissipate in an irregular, unpredictable manner. This perspective challenges neoclassical assumptions, according to which random instability, bubbles, and crashes are departures from rationality (Hu, 2025).

Building on this perspective, Gallegati and Gallegati (2025) argue that early economic approaches relied predominantly on linear models, interpreting fluctuations as minor deviations around a stable equilibrium state. Such frameworks, however, are applicable only to low-amplitude perturbations and fail to capture the complex, irregular, and aperiodic oscillations observed in real economies. Crucially, periodic systems follow regular, repeating cycles and are therefore highly predictable (Wang *et al*., 2011), whereas chaotic systems generate unpredictability through internal dynamics rather than external shocks (Chen, 2008). This distinction becomes particularly critical in carbon markets, where volatile tax regimes and evolving climate policies directly reshape the structural parameters of investment models (Zambujal-Oliveira and Duque, 2026). Carbon taxation, for instance, evolves through discrete, often unpredictable reforms rather than smooth, deterministic paths, creating incentive structures that static or continuously drifting fiscal models cannot capture. Beyond policy uncertainty, carbon credit markets are further subject to challenges in project execution, concerns over greenwashing, risks of non-equivalent credit generation, difficulties in emissions measurement, and the use of inflated baselines (Cariappa *et al*., 2024). Within such a framework, even small variations in initial conditions can be amplified through nonlinear dynamics, resulting in disproportionate and unpredictable outcomes, features that should be treated not as anomalies but as intrinsic properties of the system, underscoring the need for nonlinear analytical approaches over equilibrium-based models.

David *et al*. (2016) further emphasize that the complex behavior of real-world systems requires accurate historical modeling, as initial conditions and even small stochastic perturbations along a trajectory can substantially influence outcomes. Similarly, Cheng *et al*. (2013) argue that fluctuations in past financial variables are directly correlated with present and future volatility. In this context, the long-memory and hereditary properties inherent in economic variables make fractional-order models (Agathiyan *et al*., 2025) particularly suitable for investigating the dynamic behavior and historical dependencies of financial systems.

Adopting a deterministic chaotic framework rather than a stochastic paradigm addresses a fundamental debate in nonlinear financial literature regarding whether the irregular dynamics of environmental-economic systems stem from low-dimensional deterministic chaos or high-dimensional stochastic processes (Vogl, 2022). Although stochastic models remain the dominant convention for characterizing financial fluctuations, they are primarily descriptive rather than explanatory: they capture statistical signatures without uncovering the internal mechanisms generating such behavior. In contrast, deterministic chaotic models offer a structural perspective, demonstrating how sensitive dependence on initial conditions within a small set of nonlinearly coupled state variables can endogenously produce aperiodic, unpredictable trajectories without relying on exogenous random shocks (Chen, 2008).

Comparative empirical evidence demonstrates that low-dimensional deterministic representations can reproduce the qualitative features of financial irregularity at least as effectively as refined stochastic benchmarks, while providing superior interpretability and analytical tractability (Orlando and Zimatore, 2020; Ahmadi *et al.*, 2022). This structural tractability is central to the core objectives of the present study: the fractional-order formulation embeds long-memory properties directly through the order of differentiation rather than through an external noise term, while the deterministic state-space framework enables the synthesis of active feedback control strategies based on Jacobian linearization and Riccati equations.

Expanding on the work of Liao *et al*. (2020), subsequently analyzed by Tusset *et al.* (2023), this study applies the mathematical model proposed by those authors to investigate a carbon credit investment system. To the best of our knowledge, previous studies have not systematically explored the influence of parameters d and h on the system's dynamics. This study addresses that gap by providing a more comprehensive and rigorous characterization of the system's nonlinear dynamics, focusing on the identification of periodic and chaotic regimes. To this end, dynamic analysis tools, as discussed by Farooq et al. (2025), are employed, including phase portraits, bifurcation diagrams, time series, and the calculation of Lyapunov exponents.

In addition to characterizing the system's dynamics, this study introduces a feedback architecture capable of acting directly on the model's variables to modify and stabilize its dynamic behavior. Initially, a Linear Quadratic Regulator (LQR) controller is developed, designed based on system linearization and the solution to the algebraic Riccati equation, aiming to suppress chaotic behavior and drive state variables toward desired equilibrium values. Subsequently, to better account for the system's nonlinear characteristics, a controller based on the State-Dependent Riccati Equation (SDRE) is developed. Unlike the LQR, the SDRE allows the gain matrix to be determined as a function of the system's current state, enabling control action adapted to the nonlinear dynamics along the trajectory.

Furthermore, the study considers scenarios where not all state variables are directly available for feedback. In such cases, state observers are incorporated to estimate unmeasured variables and provide the necessary information to the LQR and SDRE controllers. A parametric sensitivity analysis is also conducted, accounting for uncertainties in model parameters, to evaluate the robustness of the control strategies against variations in system parameters. Thus, the combination of parameter characterization (parameters d and h), chaotic dynamics analysis, LQR and SDRE control strategies, state observers, and parametric sensitivity analysis enhances the understanding of the carbon credit investment system's dynamics and enables a quantitative assessment of the proposed strategies ability to stabilize the system, even in the presence of unmeasured states and parametric uncertainties.

The remainder of this article is organized as follows. Section 2 presents the mathematical model and the analytical framework adopted, covering the integer-order formulation, its extension to fractional order based on the Riemann–Liouville operator, as well as the design of the Linear Quadratic Regulator (LQR) and State-Dependent Riccati Equation (SDRE) controllers and the state observer. Section 3 presents and discusses the numerical results, including bifurcation diagrams, Lyapunov exponent maps, the analysis of fractional-order dynamics, and the performance of the proposed LQR and SDRE control strategies. Tracking errors associated with the use of observer-estimated states and the presence of parametric variations are also evaluated. Section 4 draws the main conclusions and outlines directions for future research.

2. METHODOLOGY

2.1. MATHEMATICAL MODEL

The financial system examined in this study is represented by a mathematical model with three degrees of freedom, originally proposed by Liao *et al*. (2020) and expressed by Equation (1).

$$\begin{aligned}\dot{x}_1 &= fx_3 + x_2x_1 - ax_1\\ \dot{x}_2 &= -bx_2^2 - hx_1^2 + e\\ \dot{x}_3 &= -cx_3 - gx_1 - dx_2\end{aligned} \tag{1}$$

The model captures the interaction among the carbon tax rate (x_1), the green investment demand (x_2), and the carbon price index (x_3). Parameter (a) represents the value of savings; (b) denotes the cost of green transition investment; (c) corresponds to the natural adjustment rate of the carbon price index (x3), reflecting the market's tendency to correct price deviations; and (d) measures the impact of green investment demand (x_2) on the carbon price index (x_3). Parameter (e) reflects the natural growth rate of green investment demand (x_2); (f) represents the coefficient of variation of the carbon tax rate (x_1) depending on the carbon price index (x_3); (g) denotes the sensitivity coefficient of the carbon price index (x_3) to the carbon tax rate (x_1); and (h) captures the effect of the carbon tax rate (x_1) on green investment demand (x_2).

The bifurcation diagrams with the peak displacements and the largest Lyapunov exponents were obtained using the algorithms described by Tusset *et al*. (2023).

2.2. DYNAMICAL ANALYSIS IN FRACTIONAL ORDER

As discussed by David *et al*. (2016), financial and economic variables exhibit long memory. In this context, Agathiyan *et al*. (2025) underscore that whereas integer-order models are structurally limited in capturing historical effects, fractional-order formulations explicitly embed memory of prior states. Furthermore, Tusset *et al*. (2022) highlight the application of this fractional-order perspective across a wide range of fields, thereby rendering fractional calculus a particularly suitable framework for analyzing the dynamic behavior of economic systems.

To analyze the dynamics of system (1) in fractional order, the Riemann-Liouville operator will be considered, as presented in Equation (2) (Petras, 2011; Li, 2023; Tusset *et al*., 2023):

$$D^q x(t) = \frac{1}{\Gamma(m-q)}\int_{t_0}^{t}\frac{x^{(m)}(u)}{(t-u)^{q-m+1}}du \tag{2}$$

Where $m=\lceil q\rceil$, i.e., m is the first integer not less than q. It is readily verified that this definition reduces to the classical derivative when $q=1$. The case $0<q<1$ is of particular importance. Nevertheless, there are also relevant applications for $q>1$. Without loss of generality, it is assumed throughout this work that $t_0=0,\ 0<q<1$.

The system (1) in fractional order is described by Equation (3):

$$\begin{aligned}\frac{d^{q_1}x_1}{dt^{q_1}} &= fx_3 + x_2x_1 - ax_1\\ \frac{d^{q_2}x_2}{dt^{q_2}} &= -bx_2^2 - hx_1^2 + e\\ \frac{d^{q_3}x_3}{dt^{q_3}} &= -cx_3 - gx_1 - dx_2\end{aligned} \tag{3}$$

where $0<q_1,q_2,q_3<1$, its order is denoted by $q=(q_1,q_2,q_3)$ here.

The fractional-order dynamics are investigated numerically using the algorithm proposed by Petras (2011).

2.3. DYNAMICAL ANALYSIS WITH THE INCLUSION OF CONTROL

2.3.1. LINEAR QUADRATIC REGULATOR (LQR)

According to Dörfler *et al*. (2022), the Linear Quadratic Regulator (LQR) is highly effective at mitigating system uncertainties and disturbances by optimizing performance metrics. Building on this well-established framework, the LQR is employed here to suppress the chaotic behavior of system (1), aiming to stabilize the system response and ensure robust performance in the presence of inherent noise and disturbances. Introducing the control signal U in the system (1):

$$\begin{aligned} \dot{x}_1 &= fx_3 + x_2 x_1 - ax_1 + U_1 \\ \dot{x}_2 &= -bx_2^2 - hx_1^2 + e + U_2 \\ \dot{x}_3 &= -cx_3 - gx_1 - dx_2 + U_3 \end{aligned} \tag{4}$$

The desired trajectory tracking errors are defined as:

$$\begin{bmatrix} e_1 \\ e_2 \\ e_3 \end{bmatrix} = \begin{bmatrix} x_1 - x_1^* \\ x_2 - x_2^* \\ x_3 - x_3^* \end{bmatrix} \tag{5}$$

where: x_1^*, x_2^* and x_3^* are the desired states.

Substituting Equation (5) into Equation (4), the system can be represented as:

$$\dot{\mathbf{e}} = \mathbf{Ae} + \mathbf{Bu} \tag{6}$$

where: **A** is the linearized state matrix obtained from the Jacobian matrix evaluated at the desired equilibrium.

The system (6) can be represented in the following matrix form:

$$\begin{bmatrix} \dot{e}_1 \\ \dot{e}_2 \\ \dot{e}_3 \end{bmatrix} = \begin{bmatrix} -a + x_2^* & x_1^* & f \\ -2hx_1^* & -2bx_2^* & 0 \\ -g & -d & -c \end{bmatrix} \begin{bmatrix} e_1 \\ e_2 \\ e_3 \end{bmatrix} + \begin{bmatrix} 1 & 0 & 0 \\ 0 & 1 & 0 \\ 0 & 0 & 1 \end{bmatrix} \begin{bmatrix} U_1 \\ U_2 \\ U_3 \end{bmatrix} \tag{7}$$

The control $\mathbf{U}$ is optimal and is given by:

$$\mathbf{U} = \mathbf{-R^{-1}B^{T}P\,e} = \mathbf{-Ke} \tag{8}$$

Where: $\mathbf{P}$ is the symmetric matrix and can be found from the algebraic Riccati equation:

$$\mathbf{PA} + \mathbf{A^{T}P} - \mathbf{PBR^{-1}B^{T}P} + \mathbf{Q} = \mathbf{0} \tag{9}$$

The control (8) minimizing the functional:

$$J = \int_0^\infty (\mathbf{e^{T}Qe} + \mathbf{u^{T}R\,u})dt \tag{10}$$

According to Tusset *et al*. (2023), for matrices $\mathbf{Q}$ and $\mathbf{R}$, a positive definite symmetric matrix, the matrices $\mathbf{A}$ and $\mathbf{B}$ of the system (8) are represented by:

$$\mathbf{A} = \begin{bmatrix} -a + x_2^* & x_1^* & f \\ -2hx_1^* & -2bx_2^* & 0 \\ -g & -d & -c \end{bmatrix} \text{ and } \mathbf{B} = \begin{bmatrix} 1 & 0 & 0 \\ 0 & 1 & 0 \\ 0 & 0 & 1 \end{bmatrix} \tag{11}$$

2.3.2. STATE-DEPENDENT RICCATI EQUATION CONTROL (SDRE)

The State-Dependent Riccati Equation (SDRE) technique, initially introduced in Çimen (2007) and further developed in Nekoo (2022), provides a systematic approach for designing nonlinear state-feedback controllers. The method reformulates the nonlinear system by representing its dynamics through a state-dependent coefficient matrix multiplied by the system state vector. By adopting this representation, the nonlinear characteristics of the plant can be incorporated directly into the control design while maintaining the Riccati-based formulation commonly associated with linear-quadratic optimal control. An additional advantage of the SDRE framework is the possibility of selecting weighting matrices as functions of the system states, providing greater flexibility to balance control performance, stability, and robustness according to the specific requirements of the application (Nekoo, 2022).

Considering the system with control (Equation 4), represented by the errors (Equation 5), we have system (4) represented in the following form:

$$\begin{aligned}\dot{e}_1 &= -a\,e_1 + e_1 x_2^* + e_2 e_1 + e_2 x_1^* + f\,e_3 + f x_3^* + x_1^* x_2^* - a x_1^* + U_1 \\ \dot{e}_2 &= -h e_1^2 - 2h e_1 x_1^* - b e_2^2 - 2b e_2 x_2^* - b x_2^{*2} - h x_1^{*2} + e + U_2 \\ \dot{e}_3 &= -g\,e_1 - d\,e_2 - c\,e_3 - c x_3^* - g x_1^* - d x_2^* + U_3\end{aligned} \tag{12}$$

Considering the system (5) in the following form:

$$\dot{\mathbf{e}} = \mathbf{A}(e_i)\mathbf{e} + \mathbf{BU} + \mathbf{G} \tag{13}$$

where G represents the terms that do not depend on the states and can be eliminated by considering the inclusion of a feedforward control $\mathbf{U}_{fw} = -\mathbf{G}$ (Tusset *et al.*, 2016). Including feedforward control ($\mathbf{U}_{fw}$) in the system (13), we have the following system with feedback control:

$$\begin{bmatrix}\dot{e}_1\\ \dot{e}_2\\ \dot{e}_3\end{bmatrix} = \begin{bmatrix}-a + x_2^* & e_1 + x_1^* & f\\ -h e_1 - 2h x_1^* & -b e_2 - 2b x_2^* & 0\\ -g & -d & -c\end{bmatrix}\begin{bmatrix}e_1\\ e_2\\ e_3\end{bmatrix} + \begin{bmatrix}1 & 0 & 0\\ 0 & 1 & 0\\ 0 & 0 & 1\end{bmatrix}\begin{bmatrix}U_1\\ U_2\\ U_3\end{bmatrix} \tag{14}$$

The control U is sub-optimal and is given by:

$$\mathbf{U} = -\mathbf{R}^{-1}\mathbf{B}^{T}\mathbf{P}(e_i)\mathbf{e} = -\mathbf{K}\mathbf{e} \tag{15}$$

Where: $\mathbf{P}(e_i)$ depends on the states e_i, with i=1:3, and is the symmetric matrix and can be found from the algebraic Riccati equation:

$$\mathbf{P}(e_i)\mathbf{A}(e_i) + \mathbf{A}(e_i)^{T}\mathbf{P}(e_i) - \mathbf{P}(e_i)\mathbf{B}\mathbf{R}^{-1}\mathbf{B}^{T}\mathbf{P}(e_i) + \mathbf{Q} = \mathbf{0} \tag{16}$$

The control (15) minimizing the functional (10).

2.4. CONTROL ACCOUNTING FOR OBSERVED SPACES

Considering cases where states x_1, x_2, and x_3 are unavailable and need to be estimated, one could consider including state observers in the system and using the estimated states for control.

$$\begin{aligned}\dot{\mathbf{e}} &= \mathbf{Ae} + \mathbf{Bu}\\ \mathbf{y} &= \mathbf{Ce}\end{aligned} \tag{17}$$

where **y** is the system output with the available states, and **C** is the output matrix.

Assuming that the state $\mathbf{e}$ can be approximated by the state $\hat{\mathbf{e}}$, such that (Tusset *et al.*, 2013):

$$\begin{aligned}\dot{\hat{\mathbf{e}}} &= \mathbf{A}\hat{\mathbf{e}} + \mathbf{B}\hat{\mathbf{U}} + \mathbf{K}_o\left(\mathbf{Cy} - \mathbf{C}\hat{\mathbf{y}}\right)\\ \hat{\mathbf{y}} &= \mathbf{C}\hat{\mathbf{e}}\end{aligned} \tag{18}$$

Where:

$$\mathbf{U} = -\mathbf{R}^{-1}\mathbf{B}^{T}\mathbf{P}\hat{\mathbf{e}} = -\mathbf{K}\hat{\mathbf{e}} \tag{19}$$

The matrix $\mathbf{K}_o$ can be obtained by considering the optimal feedback gain given by (Banks *et al.,* 2003):

$$\mathbf{K}_o = \hat{\mathbf{P}}\mathbf{C}\hat{\mathbf{R}}^{-1} \tag{20}$$

Where: $\hat{\mathbf{P}}$ and is obtained from the equation:

$$\hat{\mathbf{P}}\hat{\mathbf{A}}^{T} + \hat{\mathbf{A}}\hat{\mathbf{P}} - \hat{\mathbf{P}}\mathbf{C}\mathbf{R}^{-1}\mathbf{B}^{T}\hat{\mathbf{P}} + \mathbf{Q}_o = \mathbf{0} \tag{21}$$

The cost function is given by:

$$J = \int_0^{\infty} (\hat{\mathbf{e}}^{T}\mathbf{Q}_o\hat{\mathbf{e}} + \hat{\mathbf{u}}^{T}\mathbf{R}_o\hat{\mathbf{u}})dt \tag{22}$$

The matrix $\mathbf{K}_o$ is updated at each integration step when using SDRE control and is constant when using linear control.

3. RESULTS AND DISCUSSION

3.1. DYNAMIC ANALYSIS

This section presents the dynamic analysis of system (1). Numerical simulations of the system were performed using the MATLAB® ODE45 solver, based on the explicit fourth- and fifth-order Dormand–Prince Runge–Kutta method with adaptive step-size control (h = 0.01), implemented on an Intel i7 processor (3.20 GHz, six cores) with 32 GB of RAM, using the following parameters: $a = 0.3$, $b = 0.01$, $c = 1$, $e = 2.58$, $f = 2.1$, $g = 1$, and $d = [0.01{:}\,1]$ and $h = [0.02{:}\,0.2]$, with initial conditions $x_1(0) = 0.2$, $x_2(0) = 0.5$ and $x_3(0) = 0.6$.

Figure 1 shows the bifurcation diagrams for the state peaks (x_1), for the parameter ranges $d = [0.01{:}\,1]$ and $h = [0.02{:}\,0.2]$ investigated in this work. The state (x_1) was considered in the analysis, as it represents the carbon tax rate and thus plays an essential role in the investment process.

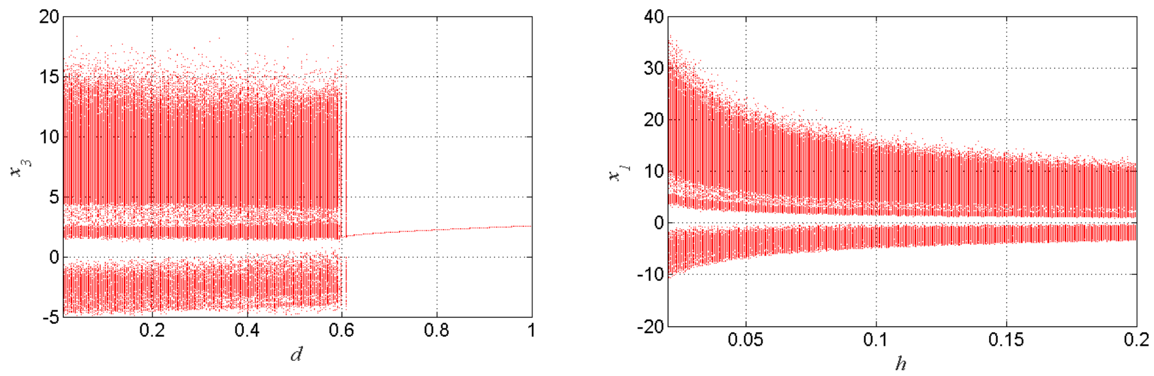

(a) (b)

Figure 1. Bifurcation diagrams. (a) $d = [0.01{:}\,1]$ versus x_1. (b) $h = [0.02{:}\,0.2]$ versus x_1.

Whereas parameter d governs transitions between chaotic and periodic regimes, parameter h does not alter the qualitative nature of the dynamics; its primary effect is on the amplitude of state variable x_1.

According to Al Dowais (2023), Lyapunov exponents quantify the average exponential rates at which neighboring trajectories diverge or converge, revealing the growth or decay of small perturbations. As Adenutsi (2025) stated, a system is chaotic when at least one Lyapunov exponent is positive, indicating high sensitivity to initial conditions. In contrast, a negative Lyapunov exponent implies that nearby trajectories stay close or converge, thereby indicating system stability. A zero exponent denotes periodic or semi-periodic behavior, meaning that trajectories maintain a constant separation over time.

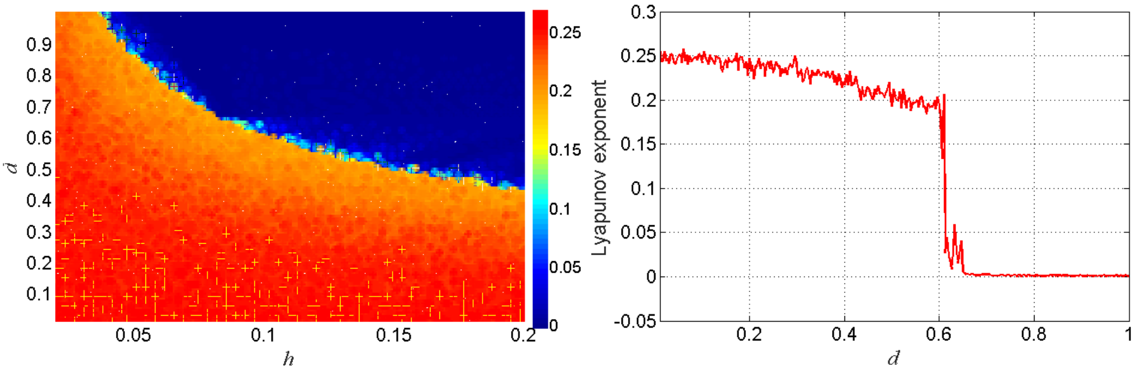

(a) (b)

Figure 2. (a) Largest Lyapunov exponent $d = [0.01:1]$ versus $h = [0.02:2]$. (b) Largest Lyapunov exponent for $d = [0.01:1]$.

As shown in Figure 2, the system exhibits periodic behavior for d<0.61 and chaotic behavior for d>0.61.

These qualitative dynamical signatures are not confined to the parameter space explored in Figure 2. Independent empirical studies of the EU ETS carbon market, analyzed from a nonlinear dynamics perspective, report a positive and large maximal Lyapunov exponent for observed European Union Allowance (EUA) price series, characterizing the market itself as "mildly chaotic" and exhibiting both market and fractal features (Feng *et al.*, 2011), consistent with the chaotic regime obtained here for d > 0.61, where the largest Lyapunov exponent likewise turns positive. Complementary evidence from the spot–futures relationship during Phase II of the EU ETS further shows that carbon allowance returns are linked asymmetrically and nonlinearly (Benz and Trück, 2009; Chevallier, 2011), reinforcing the presence of genuine nonlinear structure in real carbon markets. Taken together, these independent empirical findings lend external plausibility to the chaotic regimes identified analytically for the present model.

Figure 3 presents the time histories and phase diagrams for parameters *a = 0.3*, *b = 0.01*, *c = 1*, *d = 0.05, e = 2.58*, *f = 2.1*, *g = 1* and *h* = 0.1. These values are used throughout the remainder of the paper.

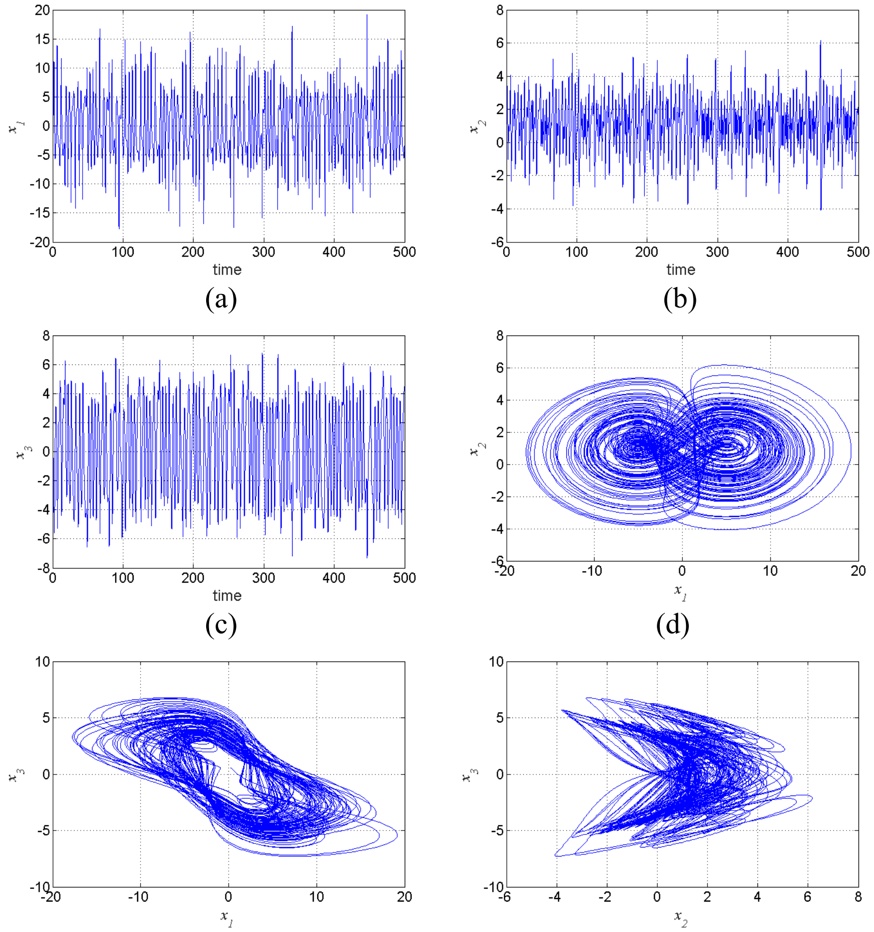

(e) (f)

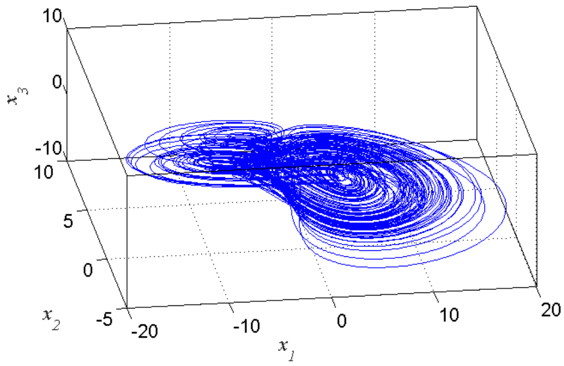

(g)

Figure 3. (a) Time histories of the state x_1; (b) Time histories of the state x_2; (c) Time histories of the state x_3. (d) Phase diagram x_1 versus x_2; (e) Phase diagram x_1 versus x_3; (f) Phase diagram x_2 versus x_3; (g) Phase diagram x_1 versus x_2 versus x_3.

As shown in Figure 3, the system exhibits chaotic behavior under the selected parameter values, which is highly undesirable for economic forecasting and investment planning.

3.2. DYNAMIC ANALYSIS OF THE SYSTEM IN FRACTIONAL ORDER

To assess the influence of memory effects on the system's behavior, the dynamics are analyzed in fractional order, thereby incorporating the hereditary properties of economic variables. Figure 4 presents the system states for different values of the fractional derivative order, with $q_1 = q_2 = q_3 = q = [0.8 : 0.999]$ considered in the simulations.

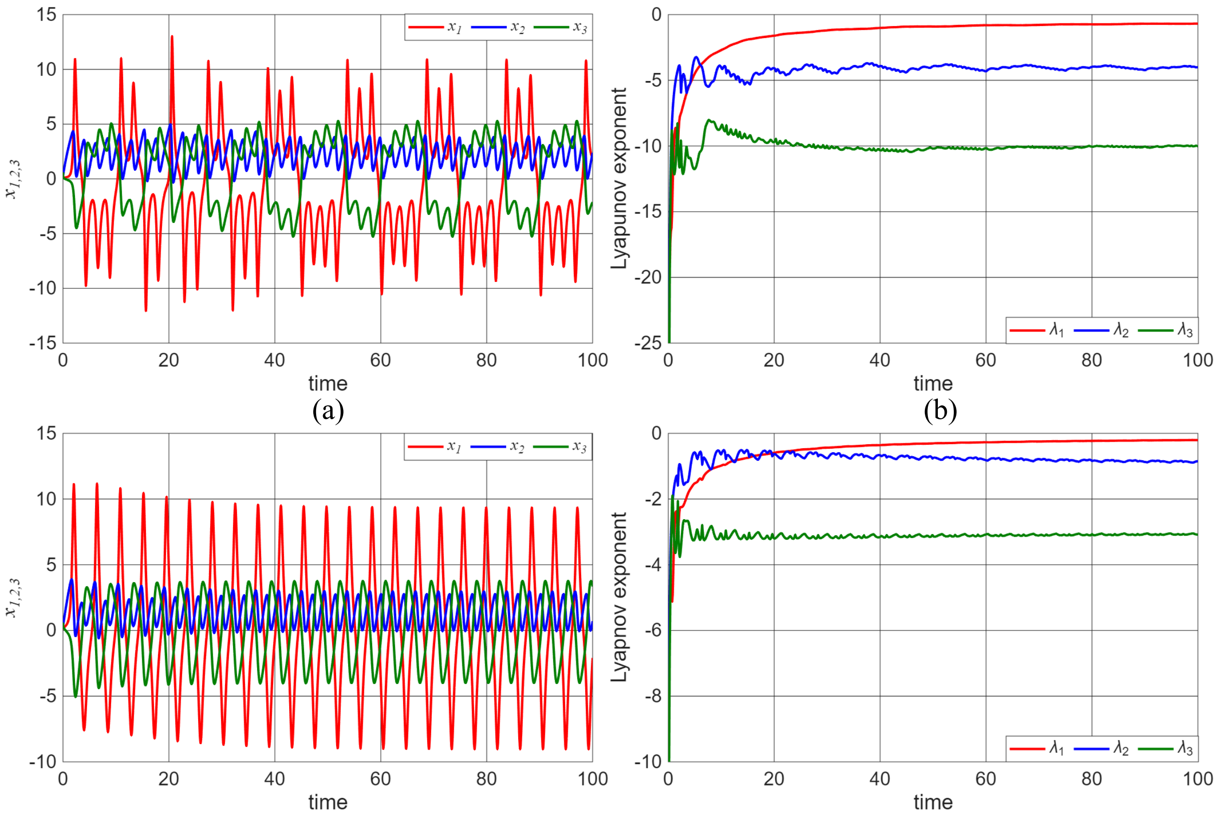

(a) (b) (c) (d)

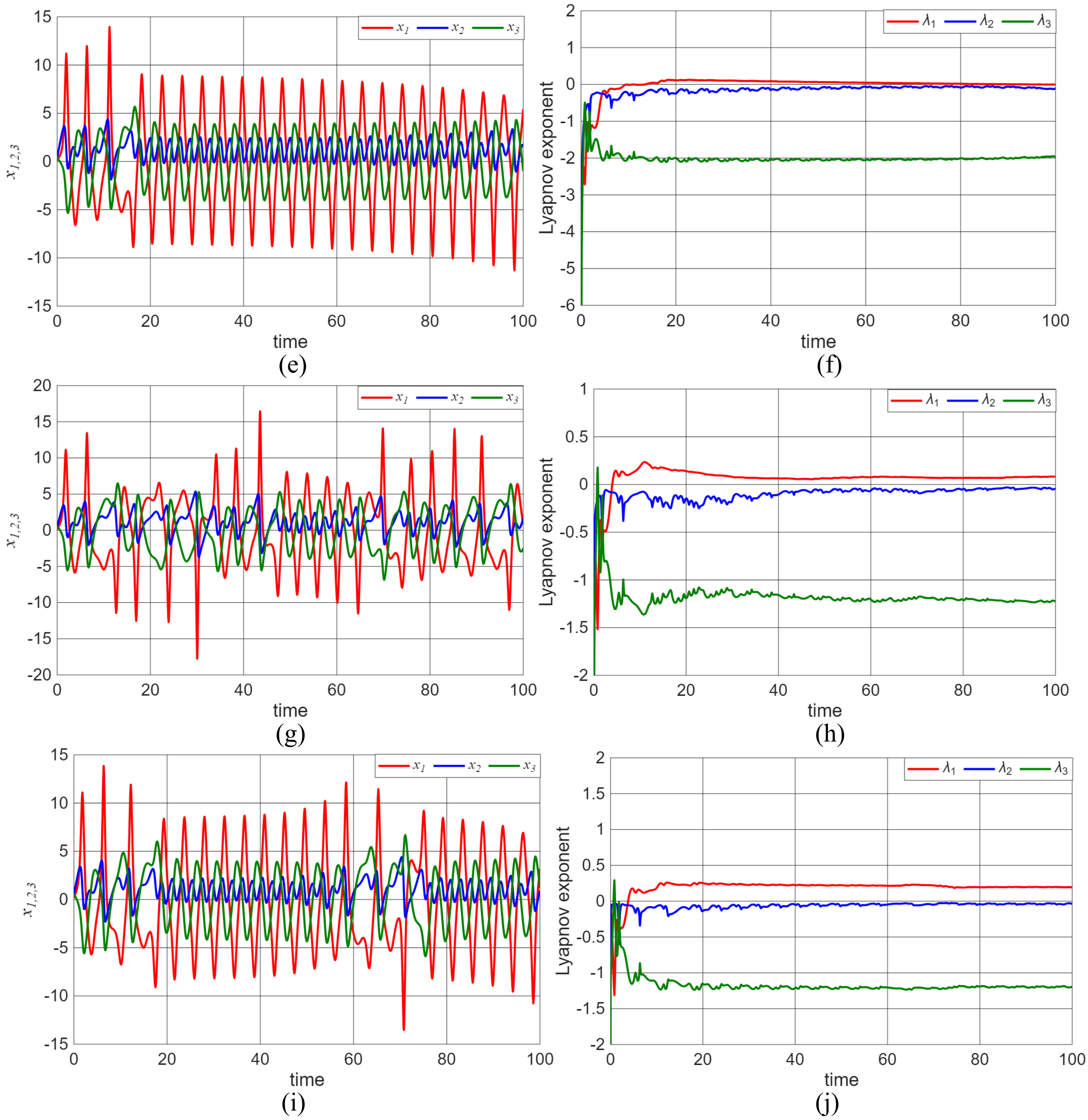

Figure 4. Time histories of the state and Lyapunov exponent, respectively. (a and b) $q = 0.80$; (c and d) $q = 0.9$; (e and f) $q = 0.95$. (g and h) $q = 0.99$; (i and j) $q = 0.999$.

As observed from the results presented in Figure 4, the system transitions to periodic behavior for q<0.99, returning to chaotic behavior for $q \geq 0.99$. Table 1 presents the variation of the three Lyapunov exponents for different values of the derivative order.

Table 1. Lyapunov exponents for variations in the order

Lyapunov exponents	$q = 0.8$	$q = 0.9$	$q = 0.95$	$q = 0.99$	$q = 0.999$
λ_1	-0.7860	-0.2053	-0.0029	0.0821	0.1937
λ_2	-4.0039	-0.8480	-0.1182	-0.0467	-0.0354
λ_3	-10.0176	-3.0817	-1.9593	-1.2213	-1.1946

As depicted in Table 1, the largest Lyapunov exponent becomes positive for q = 0.99, confirming chaotic behavior and demonstrating that the system's memory structure exerts a substantial influence on carbon credit economic forecasts, confirming that historical states and past outcomes exert a direct and persistent influence on its present and future dynamics.

As observed in Table 1, the system exhibits a transition from periodic to chaotic behavior as the fractional order varies from q = 0.95 to q = 0.99. To investigate the influence of the fractional order in greater detail, both individually and through the interaction between different orders, the system's behavior will be analyzed considering the combination of orders q = 0.95 and q = 1.

The variations in state behavior and the Lyapunov exponent are presented in Figure 5.

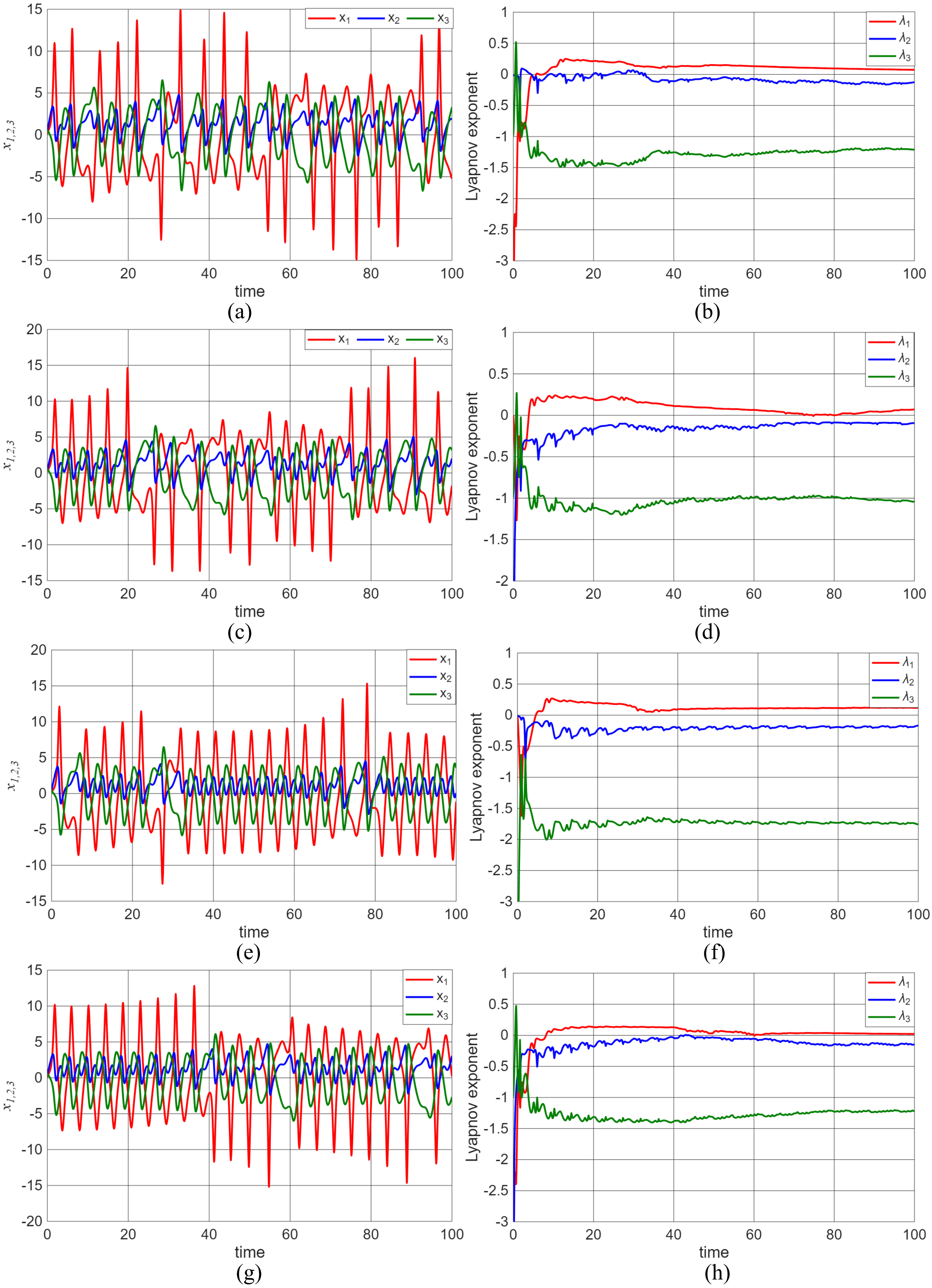

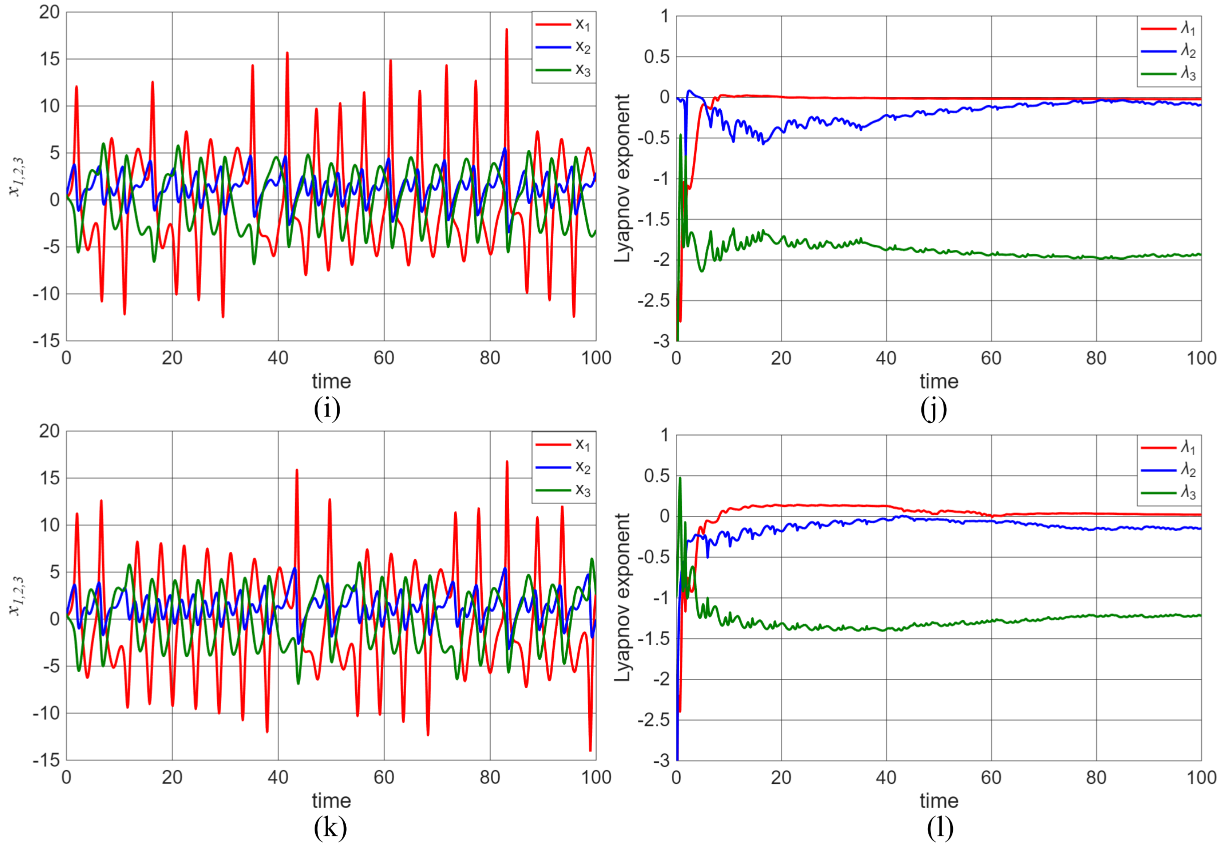

Figure 5. Time histories of the state and Lyapunov exponent, respectively. (a and b) $q_1 = 0.95$ and $q_2 = q_3 = 0.95$; (c and d) $q_1 = q_3 = 1$ and $q_2 = 0.95$; (e and f) $q_1 = q_2 = 1$ and $q_3 = 0.95$. (g and h) $q_1 = q_2 = 0.95$ and $q_3 = 1$; (i and j) $q_1 = q_3 = 0.95$ and $q_2 = 1$. (k and l) $q_1 = 1$ and $q_2 = q_3 = 0.95$.

Analysis of the results presented in Figure 5 indicates that the simultaneous variation of the fractional orders associated with variables x_1 and x_3 exerts a more significant influence on the system's dynamic behavior. It is observed that, for $q_1 = q_3 = 0.955$ and $q_2 = 1$, the system exhibits periodic behavior, demonstrating that the introduction of different fractional orders can significantly alter its dynamics. This result also suggests that the variables associated with q_1 and q_3 exert a significant memory effect on the system's evolution.

Table 2 presents the Lyapunov exponent values obtained for different combinations of fractional orders, considering $q = 0.95$ and $q = 1$. This analysis allows for a more detailed assessment of the fractional order's influence on the system's dynamics, as well as the identification of possible transitions between periodic and chaotic regimes.

Table 2. Lyapunov exponents for variations in the order q_1, q_2 and q_3.

Lyapunov exponents	$q_1 = 0.95$ $q_2 = 1$ $q_3 = 1$	$q_1 = 1$ $q_2 = 0.95$ $q_3 = 1$	$q_1 = 1$ $q_2 = 1$ $q_3 = 0.95$	$q_1 = 0.95$ $q_2 = 0.95$ $q_3 = 1$	$q_1 = 0.95$ $q_2 = 1$ $q_3 = 0.95$	$q_1 = 1$ $q_2 = 0.95$ $q_3 = 0.95$
λ_1	0.0730	0.0685	0.1187	0.0215	-0.0217	0.0184
λ_2	-0.1256	-0.0960	-0.1688	-0.1463	-0.0933	-0.1046
λ_3	-1.2127	-1.0408	-1.7559	-1.2181	-1.9342	-1.7513

As observed in Table 2, only one of the evaluated combinations results in periodic system behavior. For the remaining combinations, the integer order $q = 1$ prevails, keeping the system in a chaotic regime. This result demonstrates that the interaction between different fractional orders can play a significant role in the system's dynamics; the specific combination leading to the periodic regime suggests that memory effects associated with fractional orders can be decisive in altering dynamic behavior.

3.3. DYNAMIC ANALYSIS OF THE SYSTEM WITH THE INCLUSION OF CONTROL

3.3.1 CONTROL USING THE LQR CONTROLLER

By incorporating the proposed control (8), the desired states are initially defined as the root-mean-square (RMS) averages of the uncontrolled states x_1, x_2, and x_3 ($x_1^* = 5.03$, $x_2^* = 1.83$ and $x_3^* = 3.20$). This choice constitutes a control-theoretic feasibility benchmark rather than a policy prescription: because the RMS value represents the system's own long-run energetic average under chaotic oscillation, using it as the target demonstrates that the proposed LQR architecture can convert an intrinsically unpredictable trajectory into a stable, self-consistent equilibrium, independently of any external assumption about which equilibrium is economically or environmentally optimal. The question of which equilibrium should be targeted in practice is a distinct, policy-oriented problem.

The same control architecture developed in Section 2.3 is directly compatible with policy-anchored desired states, for instance, a carbon-price stability threshold analogous to the intervention price used by market-stabilization mechanisms in the EU Emissions Trading System, or investment-demand targets derived from sectoral decarbonization benchmarks. Translating such benchmarks into numerical targets for the present model, however, requires the states x_1, x_2, and x_3, to first be calibrated against empirical carbon market data. The RMS-based demonstration presented below should therefore be interpreted as establishing the mathematical viability of the control strategy, which can subsequently be re-parameterized with policy-derived targets once the model is empirically calibrated.

To evaluate whether the matrix (**A**), obtained through the linearization of the system, provides a controllable model for the parameters under consideration, the controllability matrix $\mathbf{M_c}$ is used. Analyzing this matrix makes it possible to determine whether the system can be driven from an initial state to any desired state through the action of the control input. Applying the controllability matrix $\mathbf{M_c}$:

$$\mathbf{M_c} = \begin{bmatrix} \mathbf{B} & \mathbf{AB} & \mathbf{A}^2\mathbf{B} \end{bmatrix} \tag{23}$$

The rank of matrix M_c is 3, demonstrating that the linearized system is controllable. Furthermore, the positive-definite matrices **Q** and **R** are defined as:

$$\mathbf{Q} = 10^3 \begin{bmatrix} 1 & 0 & 0 \\ 0 & 1 & 0 \\ 0 & 0 & 1 \end{bmatrix} \text{ and } \mathbf{R} = 10^{-3} \begin{bmatrix} 1 & 0 & 0 \\ 0 & 1 & 0 \\ 0 & 0 & 1 \end{bmatrix} \tag{24}$$

The selection of matrices **Q** and **R** was aimed at prioritizing the reduction of state variable tracking errors. The chosen **Q** matrix assigns high weight to deviations from reference states, while the **R** matrix imposes a low penalty on control effort. Consequently, the controller prioritizes system stabilization and the suppression of chaotic behavior, allowing for more intense control actions when necessary. The six-order-of-magnitude difference between the weights of **Q** and **R** reinforces this priority. Furthermore, the diagonal structure and equal weights avoid assigning greater importance to any specific economic variable. Thus, the adopted configuration ensures uniform weighting of the states and facilitates driving the economic variables toward the desired equilibrium values.

Considering the parameters: $a = 0.3$, $b = 0.01$, $c = 1$, $d = 0.05$, $e = 2.58$, $f = 2.1$, $g = 1$, $h = 0.1$, and desired states $x_1^* = 5.03$, $x_2^* = 1.83$ and $x_3^* = 3.20$. We have matrices A and P:

$$\mathbf{A} = \begin{bmatrix} 1.53 & 5.03 & 2.1 \\ -1{,}006 & -0.0366 & 0 \\ -1 & -0.05 & -1 \end{bmatrix} \text{ and } \mathbf{P} = \begin{bmatrix} 1.001526 & 0.002015 & 0.000552 \\ 0.002015 & 0.999971 & -0.000022 \\ 0.000552 & -0.000022 & 0.999001 \end{bmatrix} \tag{25}$$

Considering matrices **A**, **B**, **Q**, **R**, and **P**, we obtain the control gain matrix **K**:

$$\mathbf{K} = \begin{bmatrix} 1001.526406 & 2.015851 & 0.552135 \\ 2.015851 & 999.971509 & -0{,}022026 \\ 0.552135 & -0{,}022026 & 999{,}001506 \end{bmatrix} \tag{26}$$

Replacing the gain (14) in the control (8), we obtain the following control signals:

$$\begin{bmatrix} U_1 \\ U_2 \\ U_3 \end{bmatrix} = -\begin{bmatrix} 1001.526406 & 2.015851 & 0.552135 \\ 2.015851 & 999.971509 & -0{,}022026 \\ 0.552135 & -0{,}022026 & 999{,}001506 \end{bmatrix} \begin{bmatrix} x_1 - 5.03 \\ x_2 - 1.83 \\ x_3 - 3.20 \end{bmatrix} \tag{27}$$

Figure 6 illustrates the system response without and with control (8).

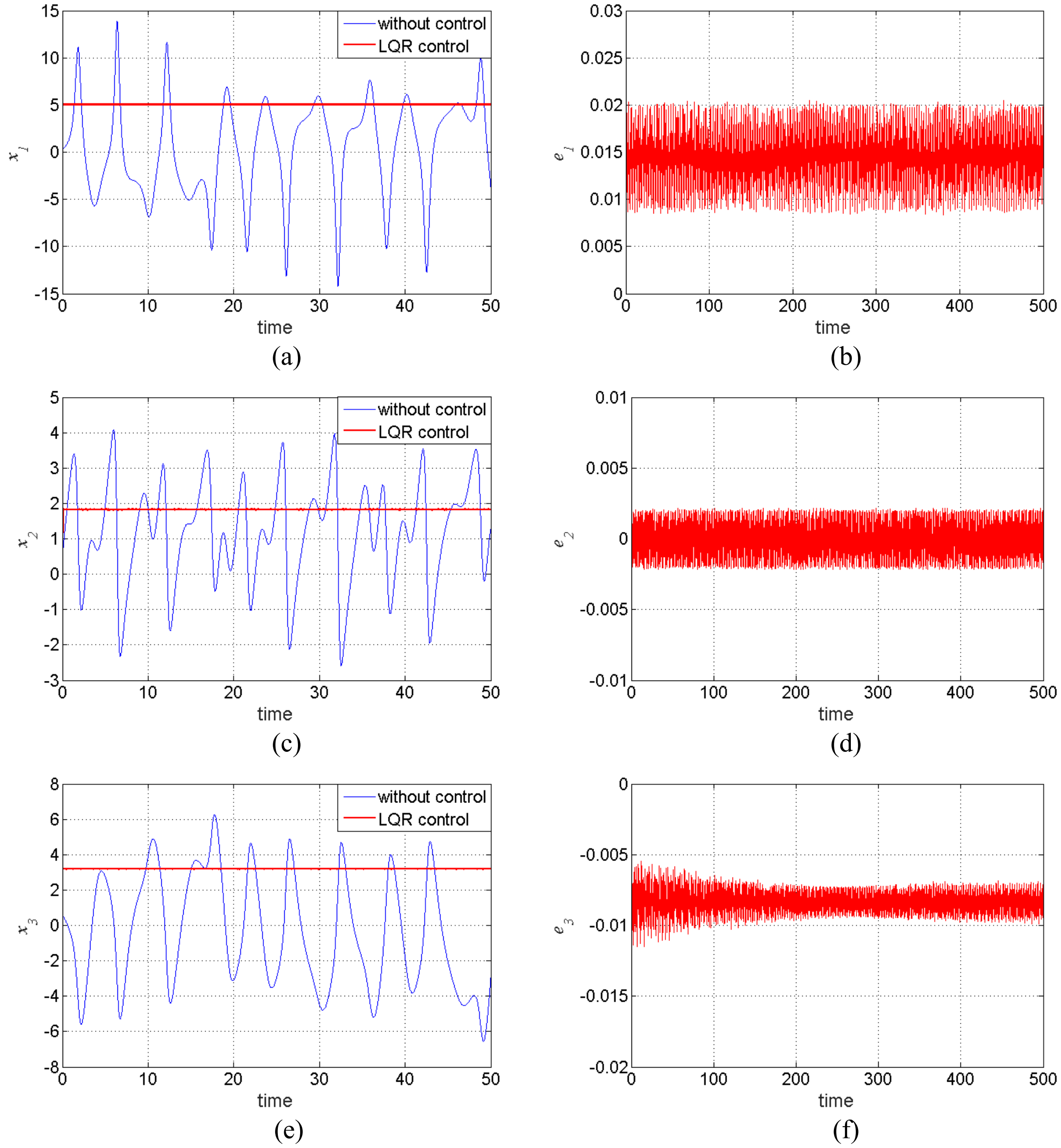

Figure 6. Application of LQR control. (a and b) Time histories of the state x_1 and $e_1 = x_1 - x_1^*$; (c and d) Time histories of the state x_2 and $e_2 = x_2 - x_2^*$; (e and f) Time histories of the state x_3 and $e_3 = x_3 - x_3^*$.

As demonstrated in Figure 6, the proposed LQR control effectively drives all state variables to their desired equilibrium values. Prior to control activation, the system exhibits persistent chaotic oscillations; once the control is engaged, convergence across all states is observed. The tracking performance is confirmed by the low RMS errors obtained: $e_{1_{RMS}} = 0.0260$, $e_{2_{RMS}} = 0.006$ and $e_{3_{RMS}} = 0.0143$, indicating that the controller is mathematically capable of suppressing the chaotic dynamics of the system. It is important to emphasize that this result establishes the theoretical stabilizability of the system rather than its operational controllability in a real policy setting.

3.3.2 CONTROL USING THE SDRE CONTROLLER

By employing the SDRE nonlinear controller, the aim is to preserve the system's nonlinear dynamic characteristics, thereby avoiding the loss of information inherent in the linearization process. Thus, unlike the linear LQR controller, whose formulation relies on a linearized model, the SDRE allows for the inclusion of state dependencies in the system representation, offering a more suitable approach for controlling nonlinear systems.

The SDRE technique to obtain a suboptimal solution for the dynamic control problem has the following procedure (Tusset *et al*., 2016):

1. Define the state-space model with the state-dependent coefficient as in Equation (14);
2. Define $e(0) = e_0$, so that the rank of $\mathbf{M_c}$ (Equation (23)) is n and choose the coefficients of weight matrices **Q** and **R**;
3. Solve the Riccati equation (16) for the state e_i;
4. Calculate the input signal from Equation (15).
5. Integrate the system (Equation (14)) and update the state e_i with these results.
6. Calculate the rank of Equation (23). If the rank equals 3, return to step 3. If the rank is less than 3, matrix A(e) is not controllable; in this case, the last controllable matrix A(e) obtained should be used, and the procedure returns to step 3.

Figure 7 presents the results obtained for the system described by Equation (14), considering the cases without control and with the application of the SDRE controller, whose control law is defined by Equation (15). This comparison allows for an assessment of the controller's influence on the system dynamics and its ability to modify the behavior observed in the uncontrolled regime.

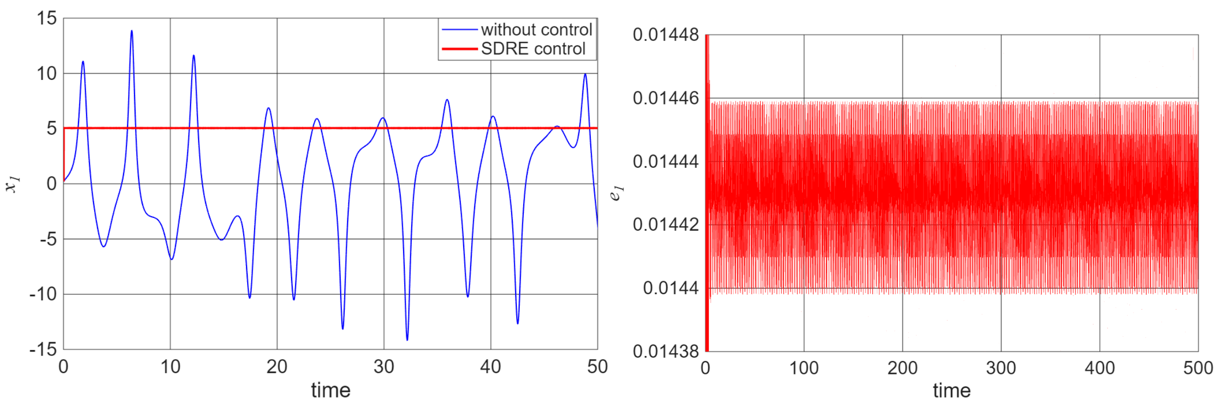

(a) (b)

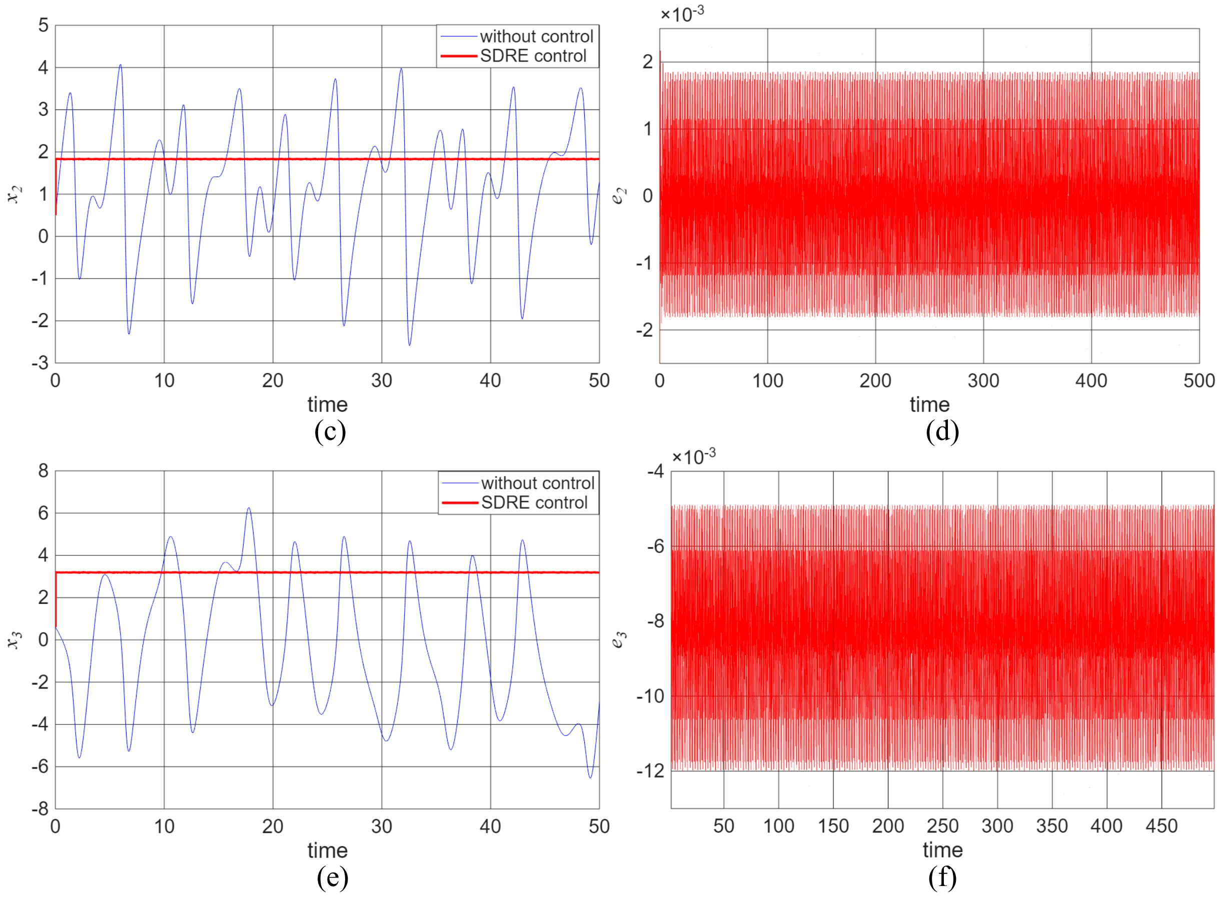

Figure 7. Application of SDRE control. (a and b) Time histories of the state x_1 and $e_1 = x_1 - x_1^*$; (c and d) Time histories of the state x_2 and $e_2 = x_2 - x_2^*$; (e and f) Time histories of the state x_3 and $e_3 = x_3 - x_3^*$.

As shown in Figure 7, the proposed SDRE controller effectively drives all state variables to their respective desired equilibrium values. Prior to the application of control, the system exhibits persistent chaotic oscillations; following controller activation, the states are observed to converge to the reference values, demonstrating the SDRE's ability to stabilize the system dynamics. Tracking performance is corroborated by the low RMS error values obtained $e_{1_{RMS}} = 0.0144$, $e_{2_{RMS}} = 0.0006$ and $e_{3_{RMS}} = 0.0084$, indicating that the controller is capable of effectively suppressing chaotic behavior and driving the system to the desired regime.

As observed with the LQR controller, it is important to note that these results demonstrate the stabilizability of the mathematical model under the conditions and parameters considered. However, this property should not be interpreted as evidence of operational controllability in a real-world carbon credit policy scenario, where economic, regulatory, and institutional factors, as well as market-related uncertainties, can significantly influence system dynamics.

3.3.3 CONTROL USING STATE OBSERVER SIGNALS

Considering situations where the states x_1, x_2, and x_3 are not directly available for feedback and therefore require estimation, state observers can be incorporated into the system, using the estimated states in the control law. This study considers the scenario in which only the carbon tax rate, x_1, is available for measurement and feedback. Thus, the variables associated with green investment demand, x_2, and the carbon price index, x_3, are estimated using state observers, as presented in Section 2.4.

Figure 8 shows the tracking errors obtained by the LQR and SDRE controllers when the estimated states x_2 and x_3 are used. For this analysis, the output matrix considered is:

$$\mathbf{C} = \begin{bmatrix} 1 & 0 & 0 \end{bmatrix} \tag{28}$$

The choice of the output matrix (Equation 28) results in the observability matrix (Equation 29) having a rank of 3, ensuring that the system is completely observable.

$$\mathbf{M}_o = \begin{bmatrix} \mathbf{C}^T & \mathbf{A}^T\mathbf{C}^T & \mathbf{A}^{T^2}\mathbf{C}^T \end{bmatrix} \tag{29}$$

The choice of matrix **C** represents the exclusive availability of variable x_1 for measurement, while x_2 and x_3 are reconstructed by the state observer and subsequently used for controller feedback.

To ensure equivalent comparison conditions between the control strategies, the following weighting matrices are considered:

$$\mathbf{Q}_o = 10^4 \begin{bmatrix} 1 & 0 & 0 \\ 0 & 1 & 0 \\ 0 & 0 & 1 \end{bmatrix} \text{ and } \mathbf{R}_o = 10^{-3} \tag{30}$$

And considering the initial conditions for the observer: $\hat{x}_1(0) = 0.15$, $\hat{x}_2(0) = 0.45$ and $\hat{x}_3(0) = 0.55$.

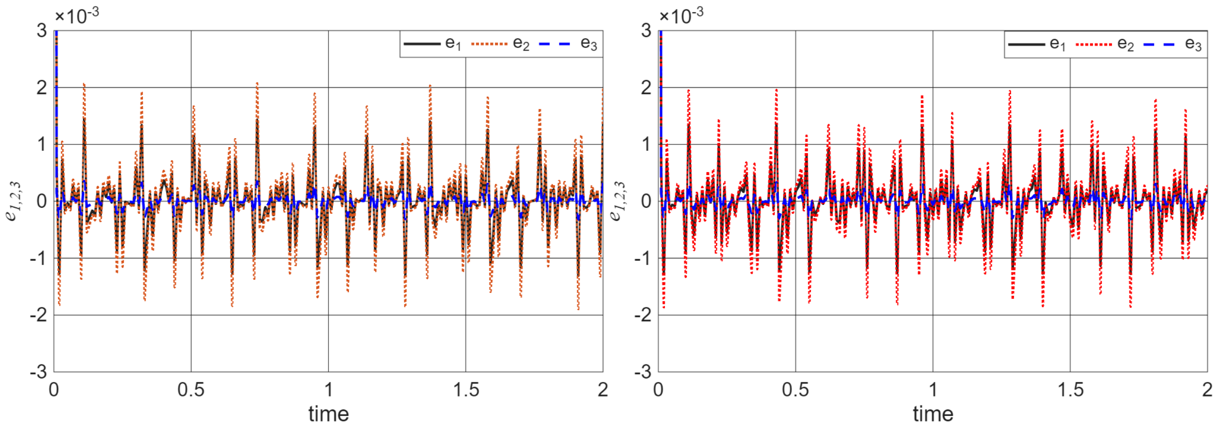

Figure 8. Errors $e_{1_{RMS}} = x_1 - \hat{x}_1$, $e_{2_{RMS}} = x_2 - \hat{x}_2$ and $e_{3_{RMS}} = x_3 - \hat{x}_3$, for the case where states x_2 and x_3 are obtained by the state observer. (a) LQR control error. (b) SDRE control error.

Table 3 presents the RMS errors obtained for each state variable, comparing controller performance when all states are directly available for feedback with that obtained when x_2 and x_3 are estimated by the state observer. This comparison allows for an assessment of the impact of using estimated states on the performance of the LQR and SDRE controllers.

Table 3. Control errors for the case where states x_2 and x_3 are estimated by a state observer.

Error	$e_{1_{RMS}} = x_1 - \hat{x}_1$	$e_{2_{RMS}} = x_2 - \hat{x}_2$	$e_{3_{RMS}} = x_3 - \hat{x}_3$
LQR	0.000519	0.0007519	0.0001273
SDRE	0.000518	0.0007518	0.0001270

As observed in Figure 8 and Table 3, the tracking errors obtained with the LQR and SDRE controllers are very close to one another, indicating that the adopted linearization preserves the system's key dynamic characteristics within the operating region considered. Furthermore, the tracking errors remain low, with values on the order of 10^{-3}. These results demonstrate that, even when using states estimated by the observer, both control strategies exhibit satisfactory performance, with negligible differences in terms of tracking precision.

3.3.4 ROBUSTNESS ANALYSIS FOR PARAMETER UNCERTAINTIES

Often, due to inherent limitations in process knowledge, the mathematical models adopted fail to accurately represent all characteristics of the system's actual dynamics. Consequently, control system performance may be compromised, as the design parameters are subject to modeling errors and uncertainties. In this context, parametric uncertainties refer to the discrepancies between the actual system parameter values and those assumed in the mathematical model. Furthermore, external disturbances and variations in operating conditions can cause changes in the parameters actually observed during system operation.

To evaluate controller robustness in the face of these uncertainties, it is assumed that model parameters are subject to random variations of up to ±20% relative to their nominal values. This approach makes it possible to assess the controllers' ability to maintain adequate performance even in the presence of parametric uncertainties and variations linked to external conditions that may affect system dynamics. Thus, the parameters used in the simulations are defined as follows: $\hat{a} = 0.3\left(0.8 + 0.4r(t)\right)$, $\hat{b} = 0.01\left(0.8 + 0.4r(t)\right)$, $\hat{c} = 1\left(0.8 + 0.4r(t)\right)$, $\hat{d} = 0.05\left(0.8 + 0.4r(t)\right)$, $\hat{e} = 2.58\left(0.8 + 0.4r(t)\right)$, $\hat{f} = 2.1\left(0.8 + 0.4r(t)\right)$, $\hat{g} = 1\left(0.8 + 0.4r(t)\right)$ and $\hat{h} = 0.1\left(0.8 + 0.4r(t)\right)$, where r(t) is a random number $r(t)$=(0, 1), with continuous uniform distribution.

Figure 9 shows the control errors caused by obtaining the control for parametric variations in the state matrix A.

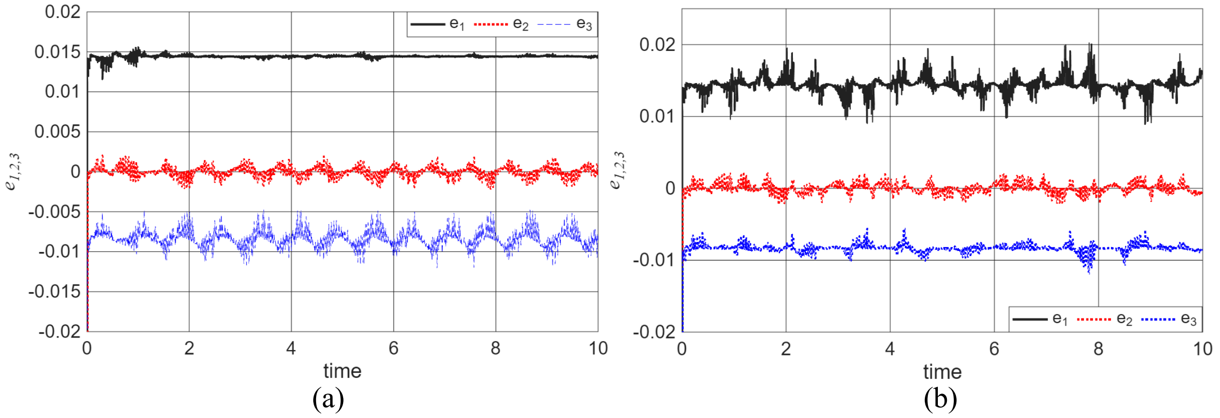

Figure 9. Errors $e_{1_{RMS}} = x_1 - x_1^*$, $e_{2_{RMS}} = x_2 - x_2^*$ and $e_{3_{RMS}} = x_3 - x_3^*$. (a) LQR control error. (b) SDRE control error.

Table 4 presents the RMS errors obtained using variable parameters in matrix (A) to evaluate the performance of the LQR and SDRE controllers in the presence of parametric uncertainties. This analysis allows for a comparison of the sensitivity of both control strategies to variations in model parameters and an assessment of their ability to maintain satisfactory performance despite the uncertainties considered.

Table 4. Control errors for the case of parametric uncertainties.

Error	$e_{1_{RMS}} = x_1 - x_1^*$	$e_{2_{RMS}} = x_2 - x_2^*$	$e_{3_{RMS}} = x_3 - x_3^*$
LQR	0.0145	0.000699	0.00835
SDRE	0.0144	0.000665	0.00843

As observed in Figure 9 and Table 4, the tracking errors obtained by the LQR and SDRE controllers are very close to one another, indicating that parametric variations affect both control strategies in a similar manner. Despite the presence of parametric uncertainties, the tracking errors remain low, demonstrating that both controllers maintain satisfactory performance in the face of the considered variations. Furthermore, the differences between the two strategies are negligible in terms of tracking precision, indicating similar behavior regarding sensitivity to parametric uncertainties.

4. CONCLUSIONS

This study investigated the dynamics of a carbon credit investment system using nonlinear analysis and fractional-order modeling. Results regarding bifurcation and Lyapunov exponents identified periodic and chaotic regimes, with a transition to chaos occurring at $d > 0.61$, while the parameter h maintained the system in a chaotic state across the analyzed range. The fractional order q also significantly influenced the dynamics, driving transitions between periodic and chaotic regimes near q = 0.99. Additionally, the simultaneous variation of the orders associated with x_1 and x_3 exerted a significant influence, highlighting the importance of memory effects on the system's dynamics.

Based on this dynamic characterization, the Linear Quadratic Regulator (LQR) and State-Dependent Riccati Equation (SDRE) controllers proved mathematically effective in suppressing chaotic behavior and driving the system to desired equilibrium states, yielding low RMS tracking errors. A comparison of the strategies revealed negligible differences in error, indicating that the linearization employed in LQR adequately preserved the system's key dynamic characteristics. Furthermore, both controllers demonstrated similar robustness when subjected to estimated states and parametric variations. However, the computational cost of LQR was approximately 98% lower than that of SDRE, as LQR utilizes a constant gain, whereas SDRE requires the gain to be updated based on the state during simulation.

It is important to highlight that the results establish the theoretical stabilizability of the system, demonstrating the existence of feedback laws capable of suppressing chaotic behavior under the conditions considered. However, the proposed controllers are formulated in continuous time and assume the availability of state variables and continuous control signal actuation, conditions that may impose limitations on their direct implementation in real-world carbon markets, where regulatory and economic decisions are made discretely and are subject to institutional, operational, and market constraints. Thus, the results should not be interpreted as a control strategy ready for implementation, but rather as a mathematical framework capable of providing relevant insights into stability, parametric sensitivity, and stabilization mechanisms. In this regard, the proposed methodology can contribute to the future development of discrete control strategies applicable to real-world scenarios, assisting policymakers and market participants in understanding and managing the complexity and volatility of carbon markets.

Future research could extend the model by calibrating parameters using real time series from carbon markets, enabling quantitative validation. Incorporating stochastic disturbances and time delays could more realistically represent market uncertainties and lags. Stochastic models and control strategies, such as LQG, could be employed to assess controller robustness. Additionally, techniques such as sliding mode control and model predictive control (MPC) could be investigated. These extensions would allow for the comparison of different strategies regarding performance, robustness, and computational cost.

AUTHOR CONTRIBUTIONS

Sofia E. Krzyuy: Conceptualization, Methodology, Investigation, Formal analysis, Data curation, Visualization, Writing – Original Draft, and Writing – Review & Editing. Giane G. Lenzi and Onelia A. A. dos Santos: Methodology, Formal analysis, and Writing – Review & Editing. Maria E. K. Fuziki: Data curation, Visualization, and Writing – Review & Editing. Angelo M. Tusset: Formal analysis and Writing – Review & Editing. Jose M. Balthazar: Supervision and Writing – Review & Editing. Leda M. S. Colpini: Conceptualization, Supervision, Project administration, and Writing – Review & Editing. All authors have read and approved the final version of the manuscript.

COMPETING INTERESTS

The authors declare that they have no known competing financial interests or personal relationships that could have influenced the work reported in this paper.

DATA ACCESSIBILITY

The authors declare that the data supporting the findings of this study are available within the paper. Further inquiries can be directed to the corresponding author.

REFERENCES

Adenutsi, D E 2025 A systems-based balanced cost-benefit analysis of corporate-community engagement in resource extraction: The CoSLIE framework. *Journal of Mathematical Finance*, 15(3): 616–665. DOI: https://doi.org/10.4236/jmf.2025.153025

Agathiyan, A, Vinothkumar, B, Akgul, A and Alshammari, F S 2025 Fractal–fractional modeling and chaos analysis of a financial system with generalized memory kernels. *Results in Control and Optimization*, 21: 100632. DOI: https://doi.org/10.1016/j.rico.2025.100632

Ahmadi, F, Aghababa, M P and Kalbkhani, H 2022 Identification of Chaos in Financial Time Series to Forecast Nonperforming Loan. *Mathematical Problems in Engineering*, 2022(1): 2055655. DOI:

https://doi.org/10.1155/2022/2055655

Al Dowais, A 2023 Differentiability of the largest Lyapunov exponent for non-planar open billiards. *Mathematics*, 11(22): 4633. DOI: https://doi.org/10.3390/math11224633

Awuah, J, Pappinen, A, Laasasenaho, K, Hassan, M K, Lauhanen, R and Kuittinen, S 2026 Evaluating the investment attractiveness and carbon credit potential of short rotation willow plantation on a cutaway peatland. *Industrial Crops and Products*, 240: 122567. DOI: https://doi.org/10.1016/j.indcrop.2025.122567

Azlen, M, Gostlow, G and Child, A 2022 The carbon risk premium. *Journal of Alternative Investments*, 25(1): 33–64. DOI: https://doi.org/10.3905/jai.2022.1.166

Banks, H T, Beeler, S C and Tran, H T 2003 State estimation and tracking control of nonlinear dynamical systems. In: Desch, W, Kappel, F and Kunisch, K (eds.) *Control and Estimation of Distributed Parameter Systems* (International Series of Numerical Mathematics, vol. 143). Basel: Birkhäuser, pp. 1–24. DOI: https://doi.org/10.1007/978-3-0348-8001-5_1

Benz, E and Trück, S 2009 Modeling the price dynamics of CO2 emission allowances. *Energy Economics*, 31(1): 4-15. DOI: https://doi.org/10.1016/j.eneco.2008.07.003

Cariappa, A A G, Konath, N C, Sapkota, T B and Krishna, V V 2024 Evaluating the potential and eligibility of conservation agriculture practices for carbon credits. *Scientific Reports*, 14: 9193. DOI: https://doi.org/10.1038/s41598-024-59262-6

Chen, W C 2008 Nonlinear dynamics and chaos in a fractional-order financial system. *Chaos, Solitons & Fractals*, 36(5): 1305–1314. DOI: https://doi.org/10.1016/j.chaos.2006.07.051

Cheng, H, Huang, J B, Guo, Y Q and Zhu, X H 2013 Long memory of price–volume correlation in metal futures market based on fractal features. *Transactions of Nonferrous Metals Society of China*, 23(10): 3145–3152. DOI: https://doi.org/10.1016/S1003-6326(13)62845-9

Chevallier, J 2011 A model of carbon price interactions with macroeconomic and energy dynamics. *Energy Economics*, 33(6): 1295-1312. DOI: https://doi.org/10.1016/j.eneco.2011.07.012

Çimen, T 2007 Approximate nonlinear optimal SDRE tracking control. *IFAC Proceedings Volumes*, 40(7): 147–152. DOI: https://doi.org/10.3182/20070625-5-FR-2916.00026

David, S A, Machado, J A T, Quintino, D D and Balthazar, J M 2016 Partial chaos suppression in a fractional order macroeconomic model. *Mathematics and Computers in Simulation*, 122: 55–68. DOI: https://doi.org/10.1016/j.matcom.2015.11.004

Dörfler, F, Tesi, P and De Persis, C 2022 On the role of regularization in direct data-driven LQR control. In: *2022 IEEE 61st Conference on Decision and Control (CDC)*. IEEE, pp. 1091-1098. DOI: https://doi.org/10.1109/CDC51059.2022.9992770

Farooq, K, Abdullah, A R, Hussain, E and Murad, M A S 2025 Chaos, Lyapunov exponent, and sensitivity demonstration of the coupled nonlinear integrable model with soliton solutions. *AIMS Mathematics*, 10(10): 22929–22957. DOI: https://doi.org/10.3934/math.20251019

Feng, Z H, Zou, L L and Wei, Y M 2011 Carbon price volatility: Evidence from EU ETS. *Applied Energy*, 88(3): 590-598. DOI: https://doi.org/10.1016/j.apenergy.2010.06.017

Gallegati, M and Gallegati, S 2025 Why does economics need complexity? *Soft Computing*, 29: 3063–3072. DOI: https://doi.org/10.1007/s00500-025-10548-5

Hu, L K 2025 Dynamic economic fluctuation with unpredictable uncertainty—some implications from the theory of complexity and chaos. *Journal of the Knowledge Economy*. DOI: https://doi.org/10.1007/s13132-025-02823-5

Johansyah, M D, Vaidyanathan, S, Hannachi, F, Sambas, A, Aruna, C and Rusyn, V 2026 Investigation of chaotic behavior, rotational symmetry, multistability and dynamic analysis for a new chaotic 4-D finance system. *Journal of Nonlinear Mathematical Physics*, 33(32): 381. DOI: https://doi.org/10.1007/s44198-026-00381-1

Li, H 2023 Determining Lyapunov exponents of fractional-order systems: A general method based on memory principle. *Chaos, Solitons & Fractals*, 168: 113167. DOI: https://doi.org/10.1016/j.chaos.2023.113167

Liao, Y, Zhou, Y, Xu, F and Shu, X B 2020 A study on the complexity of a new chaotic financial system. *Complexity*, 2020: 8821156. DOI: https://doi.org/10.1155/2020/8821156

Nekoo, S R 2022 Output- and state-dependent Riccati equation: An output feedback controller design. *Aerospace Science and Technology*, 126: 107649. DOI: https://doi.org/10.1016/j.ast.2022.107649

Okolo, C V, Susaeta, A and Sessions, J 2026 Credit market dynamics, reduced greenhouse gas, and carbon intensity targets: Insights from the Oregon clean fuels program for sustainable development. *Renewable Energy*, 256: 124489. DOI: https://doi.org/10.1016/j.renene.2025.124489

Orlando, G and Zimatore, G 2020 Business cycle modeling between financial crises and black swans: Ornstein–Uhlenbeck stochastic process vs Kaldor deterministic chaotic model. *Chaos*, 30(8): 083129. DOI: https://doi.org/10.1063/5.0015916

Petras, I 2011 *Fractional-order nonlinear systems: Modeling, analysis and simulation*. Berlin, Germany: Springer Science & Business Media. DOI: https://doi.org/10.1007/978-3-642-18101-6_3

Rigo, A, Secco, L and Pisani, E 2026 Global evidence on status, determinants, impact and barriers to adoption of agricultural carbon credits: A systematic literature review using bibliometric, TCCM and ADO framework. *Environmental and Sustainability Indicators*, 30: 101156. DOI: https://doi.org/10.1016/j.indic.2026.101156

Swinkels, L and Yang, J 2023 Investing in Carbon Credits. *Journal of Alternative Investments*, 26(2): 28–59. DOI: https://doi.org/10.3905/jai.2023.1.195

Tusset, A M, Fuziki, M E K, Balthazar, J M, Andrade, D I and Lenzi, G G 2023 Dynamic analysis and control of a financial system with chaotic behavior including fractional order. *Fractal and Fractional*, 7(7): 535. DOI: https://doi.org/10.3390/fractalfract7070535

Tusset, A M, Inacio, D, Fuziki, M E K, Costa, P M L Z and Lenzi, G G 2022 Dynamic analysis and control for a bioreactor in fractional order. *Symmetry*, 14(8): 1609. DOI: https://doi.org/10.3390/sym14081609

Tusset, A M, Piccirillo, V, Bueno, A M, Balthazar, J M, Sado, D, Felix, J L P and Brasil, R M L R F 2016 Chaos control and sensitivity analysis of a double pendulum arm excited by an RLC circuit based nonlinear shaker. *Journal of Vibration and Control*, 22(17): 3621–3637. DOI: https://doi.org/10.1177/1077546314564782

Tusset, A M, Bueno, A M, Nascimento, C B, dos Santos Kaster, M and Balthazar, J M 2013 Nonlinear state estimation and control for chaos suppression in MEMS resonator. *Shock and Vibration*, 20: 914864. DOI: https://doi.org/10.3233/SAV-130782

Verma, V 2026 Tracking Climate Finance Flows in India: The UNFCCC $100 Billion Goal. *Research and Reviews in Sustainability*, 2(1): 198–217. DOI: 10.65582/rrs.2026.013

Vogl, M 2022 Controversy in financial chaos research and nonlinear dynamics: A short literature review. *Chaos, Solitons & Fractals*, 162: 112444. DOI: https://doi.org/10.1016/j.chaos.2022.112444

Wang, Z, Huang, X and Shi, G 2011 Analysis of nonlinear dynamics and chaos in a fractional order financial system with time delay. *Computers & Mathematics with Applications*, 62(3): 1531–1539. DOI: https://doi.org/10.1016/j.camwa.2011.04.057

Xi, J, Boateng, S A, Karikari, F A, Khan, S, Sackitey, G M and Fumey, M P 2026 Financial markets and renewable energy transitions: Evidence from energy investment, domestic credit, market capitalisation and institutional quality. *Energy*, 346: 140286. DOI: https://doi.org/10.1016/j.energy.2026.140286

Xu, L, Solangi, Y A and Wang, R 2023 Evaluating and prioritizing the carbon credit financing risks and strategies for sustainable carbon markets in China. *Journal of Cleaner Production*, 414: 137677. DOI: https://doi.org/10.1016/j.jclepro.2023.137677

Zambujal-Oliveira, J and Duque, J 2026 Stochastic carbon taxes and capital turnover: A real options model for decarbonization investment. *Results in Engineering*, 29: 109902. DOI: https://doi.org/10.1016/j.rineng.2026.109902

Zhang, X, Xie, X, Xiao, J and Wang, Y 2025 Green credit and enterprises' carbon emission intensity: empirical data from Chinese microenterprises. *Scientific Reports*, 15(1): 1–16. DOI: https://doi.org/10.1038/s41598-025-98139-0

Zhen, D, Wu, X, Liu, K, Ji, Y, Xiong, C and Cui, Q 2026 Carbon credit in travel demand management: an incentive-based framework for emission reduction. *Transportation Research Part D: Transport and Environment*, 150: 105041. DOI: https://doi.org/10.1016/j.trd.2025.105041